Indian Journal of Biochemistry & Biophysics
Vol. 59, July 2022, pp. 755-766

Biomimetic of hydroxyapatite with *Tridax procumbens* leaf extract and investigation of antibiofilm potential in *Staphylococcus aureus* and *Escherichia coli*

Anusuya Nagaraj[1], Naveen Kumar Kalagatur[2], Krishna Kadirvelu[2], Sushmitha Shankar[3], Usha Kiranmayi Mangamuri[4], Sudhakar Poda[4] & Suja Samiappan[1]*

[1]Department of Biochemistry, Bharathiar University, Coimbatore- 641 046, Tamil Nadu, India
[2]DRDO-BU-Center for Life Sciences, Coimbatore-641 046, Tamil Nadu, India
[3]Department of Biotechnology, University of Mysore, Mysuru-570 005, Karnataka, India
[4]Department of Biotechnology, Acharya Nagarjuna University, Guntur- 522 510, Andhra Pradesh, India

Received 08 March 2022; *revised 23 July 2022*

In the last few decades, hydroxyapatite (HA) has become one of the most highly prized biominerals in the biomedical industry for orthopedic and dental applications. The focus of this research was to synthesize biomimetic HA from *Tridax procumbens* (TP) leaf extract and investigate their antibiofilm properties. The HA was made using the sol-gel method and the HA-TP biocomposite was made by precipitation method. The d.nm size of HA and HA-TP biocomposite was determined as 193.28 and 258.14 d.nm, respectively. The zeta potential of HA and HA-TP biocomposite was determined as −21.2 and −18.3 mV, respectively, and found highly stable. The FTIR study revealed that phytochemicals of TP were successfully impregnated into HA-TP biocomposite. The HA and HA-TP biocomposite were found spherical and agglomerated from SEM analysis. In HR-TEM analysis, the average diameter of the HA and HA-TP biocomposite were 16.57 – 64.22 nm and 51.71 – 138.68 nm, respectively. According to the EDX analysis, HA is primarily composed of calcium, oxygen, and phosphate, whereas, HA-TP biocomposite is primarily composed of calcium, phosphate, oxygen, and carbon. In the antioxidant assay, the IC_{50} value (concentration required to scavenge 50% of free radicals) of HA-TP biocomposite was determined as 156.69 ± 14.02 and 180.21 ± 12.84 µg/mL in DPPH and ABTS free radical scavenging assays, respectively. The MIC (minimum inhibitory concentration) and MBC (minimum bactericidal concentration) of as-synthesized HA-TP biocomposite against *Staphylococcus aureus* – ATCC 13565 and *Escherichia coli* – MTCC 41 were observed as 181.09 ± 21.47 and 317.30 ± 41.03, and 157.59 ± 32.18 and 264.03 ± 21.58 µg/mL, respectively. The as-synthesized HA-TP biocomposite has detrimentally affected the biofilm formation of both the tested bacteria *S. aureus* – ATCC 13565 and *E. coli* – MTCC 41. The study concluded that the as-synthesized HA-TP biocomposite could be highly helpful in the biomedical field for alleviating oxidative-stress-related disorders and inhibiting microbial biofilm formation.

Keywords: Antioxidant activity, Biocomposite, Biofilm, Hydroxyapatite, *Tridax procumbens*

For the last ten decades (1920), researchers have concentrated their research efforts on designing and producing artificial bone with the intent of developing functional bone regeneration alternatives[1]. Later phase in the 1960s, development in biomaterial science was mostly linked with progress in artificial bone materials, which mostly focused on the utilization of bioactive or biodegradable materials. During this era, second-generation biomaterials known as bioactive ceramic materials emerged *e.g*., hydroxyapatite (HA). HA is made up of calcium phosphates, which are the most important biominerals in animals. The HA biomaterials have significant advantages, including biocompatibility, conveniently configurable physical-chemical characteristics, inertness, high toughness, and resistance to degradation[2]. Since the 1980s, HA has acquired a lot of interest from scientists and experts in the healthcare profession and has appealed to a lot of interest in the biomedical field, such as orthopedics and dental implants because the features of HA are equal to those of the human skeleton[3]. In recent times (from 2000), bioceramics have taken on a new dimension thanks to advances in manufacturing technologies, such as nanotechnology and a decent grasp of regenerative science. HA is one of the bioceramics that makes up the vast majority of the regenerative graft material available in the market. Because of its properties, HA is gaining popularity in regenerative medicine as a viable alternative material

*Correspondence:
E-mail: suja.s@buc.edu.in

for autograft. In the future, the innovative application of HA could be a boon by nanotechnology. The fascinating developments for HA on an industrial scale include applications in drug targeting, 3-D cell and tissue culture, scale-up of production, and purification antibodies for diagnostics and therapeutics[4].

Investigations revealed that HA has a high affinity for a wide range of proteins, nucleotides, and lipids; regrettably, this affinity trait makes HA a much more suitable site for microbial invasion, formation of biofilms, and the synthesis of endotoxins[5]. Bacterial pathogens are the causative factors of human illnesses and are one of the most serious health risks[6]. Biofilm formation is linked to 65 to 80% of bacterial illnesses, according to data from the Centers for Disease Control and Prevention (CDC) and the National Institutes of Health (NIH). In unfavorable conditions, the biofilm acts as a protective covering for the bacteria, as well as a shield for antibiotics, preventing antibiotics from reaching the bacterium, ensuing in the ongoing development and the formation of a mature biofilm. Furthermore, by generating superantigens within the biofilm, these mature biofilm bacteria can infect the immune system. They're considered to be a key pathogenicity factor that leads to recurring and chronic illnesses. When compared to planktonic or free-floating bacteria, bacteria that live in a biofilm matrix are more antibiotic-resistant (10-1000 times). Biofilms, in general, protect planktonic bacteria from the host's immune system by preventing the complement system and phagocytes from becoming activated. As a result, biofilms pose a major risk to the biological and healthcare domains[7].

As a result, understanding how to successfully treat biofilms is critical for reducing the risk of reinfection and improving treatment efficacy. As a result, the use of HA fortified with metallic ions is the most recent and cutting-edge strategy in the modern field of nanoscience to improve antibacterial performance in orthopedics, particularly in bone tissue formation, osteoconductive and osteointegration effects, and dentistry[8]. Even though doped metal ionic HA has a good effect in biomedicine, it also causes detrimental metal toxicity by aggregating into soft tissues such as the kidneys, hepatic, and lungs, resulting in muscular pseudocapsules due to the contrast among antioxidants and oxidants[9]. As a result, there is a growing demand for nanoparticle synthesis techniques that are clean, non-toxic, and environmentally friendly (green nanotechnology)[10-14]. Accordingly, a major area of research interest in the current environment is scaling up naturally occurring plant-derived extracts capable of inhibiting biofilm formation. Thus, a new insight into the antagonistic impact of medicinal plant materials biomimetic with HA on bacterial pathogens could be considered a more effective and alternative candidate for biomedical treatments[15].

In the present study, HA was biomimetic with leaf extract of *Tridax procumbens* (TP) and explored antibiofilm activities. Dexamethasone, luteoline, glucotureolin, β-sitosterol flavone, glycoside, sterols, flavonoids, polysaccharides, and bergenin derivatives were found to be abundant in TP extracts[16]. Typhoid fever, flu, cough, epilepsy, bronchitis, and dysentery have all been treated with TP in the past. TP is reported to have antioxidant, anti-inflammatory, immunomodulatory, hepatoprotective, anti-diabetic, hemostatic, antipyretic, and antimicrobial potential[17].

In the contemporary research, HA was prepared from calcium nitrate tetrahydrate and orthophosphoric acid by sol-gel technique and followed by biomimetic of HA was done with leaf ethanolic extract of TP. Following, physico-chemical properties of the as-synthesized HA and biomimetic HA-TP biocomposite were characterized by XRD, FTIR, Zeta potential, and size distribution, SEM with EDX, and HR-TEM analysis. Further, oxidative stress eliciting free radicals quenching antioxidant potentials of HA-TP biocomposite was revealed by *in vitro* DPPH and ABTS assays. In the final study, the antibacterial activity of HA-TP biocomposite against *Staphylococcus aureus* – ATCC 13565 *and Escherichia coli* – MTCC 41 was revealed by the micro-well dilution technique. The antibiofilm activity of HA-TP biocomposite against *S. aureus* – ATCC 13565 and *E. coli* – MTCC 41 was revealed by crystal violet staining.

Materials and methods

Chemicals and reagents

Sodium carbonate, Folin-Ciocalteu reagent, aluminum chloride, sodium nitrite, sodium hydroxide, calcium nitrate tetrahydrate (CNT), ortho-phosphoric acid (O-PA), ammonia, potassium persulfate, potassium ferric cyanide, ferric chloride, Muller-Hinton broth (MHB), tryptic soy broth, Muller-Hinton agar (MHA), tetracycline, saline, nutrient broth, and crystal violet were received from HiMedia (Mumbai, India). Gallic acid, tannic acid, quercetin, 2,2-

diphenyl-1-picrylhydrazyl (DPPH), ascorbic acid, and 2,2'-azino-bis(3-ethylbenzothiazoline-6-sulfonic acid) (ABTS) were purchased from Sigma-Aldrich (Bangalore, India). Ethanol, methanol, and other reagents used in the study belonged to analytical grade and were obtained from Merck, Bengaluru, India.

Collection and extraction of plant material

The leaves of *Tridax procumbens* (TP) were collected from Bharathiar university campus, Coimbatore, Tamil Nadu, India. The plant voucher was confirmed and safeguarded. The fresh and healthy leaves of TP were separated and washed with double distilled water 2-3 times to assure that the dirt on their surface was eliminated. The leaves were then dried for one week in the shade at ambient temperature. The dried leaves were finely pulverized in an electrical grinding device. Following, TP leaves powder (10 g) was dissolved in 100 mL of ethanol adopting the cold maceration technique. The maceration process was continued for three days before being filtered through Whatman® grade 1 filter paper and lyophilized at −39°C to concentrate the phyto ingredients enriched filtrate. The obtained TP extract was stored at 4°C in a sterile airtight pack and used for further studies.

Determination of total phenolics, flavonoids, and tannins content

The total phenolics, flavonoids, and tannins of TP extract were done as per the methodology of Kalagatur *et al.*[18] and Gunti *et al*[19]. The total phenolics, flavonoids, and tannins of TP extract were expressed as milligrams of gallic acid, quercetin, and tannic acid equivalents per gram of TP extract.

Synthesis of HA and HA-TP biocomposite

Calcium nitrate tetrahydrate (CNTH), phosphoric acid (PA), and ammonia solution were used as precursors in the synthesis process of hydroxyapatite (HA). In double distilled water, 0.25 M PA was prepared and ammonia solution was used to adjust the pH of the solution to 10. Separately, 1 M CNTH was prepared in double-distilled water, and drop by drop the prepared CNTH solution was added to the earlier prepared PA-ammonia solution, retaining the Ca/P ratio at 1.67. A steady stream of ammonia solution was introduced to keep the pH at 10 until the CNTH solution was fully incorporated. The produced solution was vigorously agitated for 1 hr and then aged for 24 h at room temperature. The mixture formed into a gel after 24 h. This gel was dried in a hot air oven at 65°C, then washed 3–4 times in distilled water. To obtain HA powder, the powder was dehydrated in the oven and then heat-treated (calcination) in an electrical furnace at 800°C for 1 h[20].

Adopting the precipitation process, the HA-TP biocomposite was synthesized. First, HA was slowly dispersed in 50 mL of ethanol, and TP extract was added to the solution and retained for gentle mixing under 80 rpm overnight to ensure that all particles between the HA and TP were evenly mixed. The precipitated solution of the HA and TP was dried in an oven at 35°C for 24 h. The dried sample was then pulverized and sieved to obtain the fine powder.

Characterization of HA and HA-TP biocomposite

Zetasizer Nano ZS (Malvern, USA) was used to perform dynamic light scattering (DLS) analysis to determine the hydrodynamic diameter of the as-synthesized HA and HA-TP biocomposite. The polydispersity index and zeta potential (charge) were also calculated using Zetasizer Nano ZS (Malvern, USA). FTIR 84005 (Shimadzu, Tokyo, Japan) with ATR mode was used to identify the functional groups present in the produced HA and HA-TP biocomposite. One percent of the powder was blended and mashed with 99% KBr and the spectra were captured in the range of 400 to 4000 cm^{-1}. Cu Kα radiation (k = 0.15406 nm) was used to detect the crystalline phase of HA and HA-TP biocomposite using an X-ray powder diffractometer (XRD; Geiger Flex, Rigaku) with a voltage of 30 kV and a current of 20 mA. The specimens were scanned at a speed of 0.05°/s in a range of 10° to 80°. The micro-morphology and chemical make-up of HA and HA-TP biocomposite was correspondingly examined with a scanning electron microscope (SEM) and energy dispersive X-ray analysis (EDX) (FEI, Quanta 200, Thermo Fisher Scientific, USA) at a 15-20 kV. The size and morphology of the HA and HA-TP biocomposite were determined using a JEOL JEM 2100, HR-TEM (Tokyo, Japan) at an accelerating voltage of 200 kV[15,19].

Antioxidant potential of HA-TP biocomposite

The antioxidant potential of HA-TP biocomposite was determined by DPPH and ABTS assay. With slight changes, the ABTS radical scavenging activity of HA-TP biocomposite was tested using Kumar *et al*., approach[21]. In brief, 0.7 optical density ABTS (7 mM)

solutions were prepared in 2.4 mM potassium persulfate solutions and added to various amounts of HA-TP biocomposite, incubated at room temperature for 10 min in the dark, and optical density was measured at 730 nm using a microplate reader (Synergy H1, BioTek, USA). Ascorbic acid was employed as a standard reference, and the reaction combination without HA-TP biocomposite was used as a control.

With a few modifications, the 2,2-diphenyl-1-picrylhydrazyl (DPPH) radical scavenging activity of HA-TP biocomposite was measured using the Kalagatur *et al*., approach[22]. The total volume was adjusted to 3 mL with methanol after 0.5 mL of methanolic DPPH (0.1 mM) and 1 mL of 0.1 M acetate buffer were blended with different volumes of HA-TP biocomposite. The optical density of the combination was measured at 515 nm after 20 min at room temperature. Ascorbic acid served as a standard reference, while the reaction combination in the absence of HA-TP biocomposite served as a control.

The study's findings were expressed as an IC_{50} value. The IC_{50} value was calculated as the amount of HA-TP biocomposite necessary to lower the oxidant solution's (ABTS or DPPH radical solution) optical density by 50%.

$$\text{ABTS or DPPH radical scavenging potential (\%)} = \frac{(A_c - A_t)}{A_c} \times 100$$

In the equation, the terms 'A_t' and 'A_c' correspond to the absorbance of the test and control samples.

Antimicrobial activity of HA-TP biocomposite

In the present study, the antibacterial activity of HA-TP biocomposite was determined against *S. aureus* – ATCC 13565 and *E. coli* – MTCC 41. Bacterial cultures were received from DRDO-BU Center for Life Sciences, Coimbatore, India. Bacteria were cultivated for 24 h at 37°C in a nutrient broth, and their growth was assessed using a microplate reader at 600 nm (Synergy H1, BioTek, USA). The optical density of bacterial culture was adjusted to 0.5 McFarland standard in sterile saline (pH 7.4). Micro-well dilution and anti-biofilm assays were used to determine the antibacterial efficacy of HA-TP biocomposite.

Micro-well dilution technique

The antimicrobial activity of HA-TP biocomposite was assessed by micro-well dilution technique adopting the technique of Kalagatur *et al*., with minor modifications[23]. Briefly, in a 96-well plate, HA-TP biocomposite at various concentrations (up to 350 µg/mL) and an overnight bacterial culture of 0.5 McFarland (10 µL) was added, and the final volume was adjusted to 100 µL with MHB and incubated at 37°C for 24 h. Following, optical density was recorded at 600 nm using a microplate reader (Synergy H1, BioTek, USA). A minimal inhibitory concentration (MIC) of HA-TP biocomposite was found to be the concentration of the HA-TP biocomposite at which there was no increase in optical density (bacterial growth). Furthermore, 10 µL was taken from 96-well plate wells and spread out on MHA Petri plates, which were then incubated for 24 h at 37°C. The concentration of HA-TP biocomposite at which there was bacterial growth not detected was determined as minimum bactericidal concentrations (MBC). In the investigation, tetracycline was used as a standard antibacterial agent. The wells that were not treated with HA-TP biocomposite or tetracycline were referred to as the control wells.

Antibiofilm activity

Antibiofilm activity of HA-TP biocomposite was carried out by methodology of Li *et al*. with minor modifications[24]. In brief, different concentrations of HA-TP biocomposite (up to 350 µg/mL), 10 µL of an overnight bacterial culture of 0.5 McFarland, and the total volume were adjusted to 250 µL with tryptic soy broth and properly mixed in 24-well plates. Following that, the test plates were incubated at 37°C in a static condition for 24 h. As a positive control, tetracycline was utilized. Control wells were those without HA-TP biocomposite and antibiotic.

After incubation, the contents of the plates' wells were removed, and the wells were gently washed with saline, to remove non-adherent free-floating bacteria. The wells of the plates were then air-dried for 30 min. Following drying, adhering "sessile" bacteria in the wells were fixed with 2% *w/v* sodium acetate, then stained with 0.1% *w/v* crystal violet dye and incubated in the dark for 30 min. To remove any remaining dye, the wells were thoroughly cleaned with sterile distilled water. The plates were then air-dried and suspended in distilled water, and images were obtained using microscope (EVOS FLC, Thermo Fisher Scientific, USA). Following that, distilled water was discarded, the wells were dried for 30 min, 100 µL of ethanol (95% *v/v*) was added to each well, and the absorbance at 620 nm was measured using a microplate reader (Synergy H1, BioTek, USA). The proportion of

biofilm growth suppression by HA-TP biocomposite was calculated using the following equation:

$$\text{Biofilm inhibition activity (\%)} = \frac{(A_c - A_t)}{A_c} \times 100$$

In the equation, the terms 'A_t' and 'A_c' correspond to the absorbance of the test and control samples.

Statistical analysis

The experiments were carried out in six replicates (n = 6) independently, and the data were expressed as mean standard deviation. Following the Student's *t*-test, the collected data were analyzed using one-way ANOVA. A *P*-value $\leq$ 0.05 was used to define statistical significance.

Results and Discussion

Phytochemical profile of TP extract

For more than 80% of the world's population, plants and herbal therapies are claimed to be the primary source of health care. The numerous health benefits of herbs are due to the considerable levels of active metabolites. As a result, TP leaves were obtained, extracted, and used in this research. Phytochemical investigations were used to determine the types of phytochemicals (phenolics, flavonoids, and tannins) contained in the ethanolic leaf extract of TP.

Phenolic chemicals are involved in defense systems and have been linked to improved health. Phenolic chemicals act as an antioxidant and protect against microbial infections, assisting in the prevention of chronic and infectious disorders. Inactivating lipid free radicals or inhibiting the breakdown of hydroperoxides (hydrogen peroxide) into free radicals were linked to phenolics' antioxidant action[25]. Similarly, Flavonoids are a type of polyphenol found in fruits, leaves, vegetables, and other plant parts, and they've been associated with a lower risk of major degenerative diseases. Flavonoids contain antioxidant properties, which may help to reduce cellular oxidative stress[26,27]. Tannins are naturally occurring phenolic chemicals that are found in almost every plant. Fruits, timber, and bark of trees, as well as many types of wild herbs and plants contain them. Medical and pharmacological properties revealed that tannins are highly potential in healing or alleviating a range of illnesses and disorders[28].

In the present study, total phenolic, flavonoid, and tannin content were determined by Folin-Ciocalteu, aluminum chloride, and ferric chloride methods, respectively. One gram of TP extract was found to have a total phenolic, flavonoid, and tannin content of 12.46 ± 0.23 mg gallic acid equivalent, 10.07 ± 0.30 mg quercetin equivalent, and 2.04 ± 0.09 mg tannic acid equivalent, respectively. According to the findings, an ethanolic TP extract is appropriate for the fabrication of HA biocomposite, and thus, HA-TP biocomposite could be extremely beneficial in using the antioxidant potential for the treatment of oxidative stress illnesses. In addition, the HA-TP biocomposite may be useful in preventing microbial infections from forming biofilms.

Synthesis and characterization of HA and HA-TP biocomposite

CNT and OPA are the chemical precursors used in this study to fabricate HA material in an alkaline environment. Following that, the green template for HA-TP biocomposite synthesis was executed by green source enriched bioactive molecules from TP ethanolic extract by precipitation technique. The as-synthesized HA and HA-TP biocomposite were evaluated using various nanotechnology techniques.

Size distribution of HA and HA-TP biocomposite was measured by DLS analysis. The d.nm size of HA and HA-TP biocomposite was determined as 193.28 and 258.14 d.nm, respectively (Fig. 1A & B). The polydispersity index for HA and HA-TP biocomposite was determined to be 0.188 for HA and 0.297 for HA-TP biocomposite. Due to the presence of capping and reducing agents in the TP, the obtained data index demonstrated a low agglomeration in the HA-TP biocomposite.

The zeta potential of nanoparticles is a measurement of their surface charge. The surface charge of a particle reflects how stable it is in a suspension system. In the present study, HA and HA-TP biocomposite exhibited good zeta potential of −21.2 and −18.3 mV, respectively (Fig. 1C & D). According to the findings, as-synthesized HA and HA-TP biocomposite were very stable in solution form and might retain their potential benefits for a longer period.

The success of TP extract impregnation into HA-TP biocomposite was determined by FTIR analysis. The functional groups present in the HA, TP, and HA-TP biocomposite synthesized in the presence of TP bioactive metabolites were determined by FTIR spectra, and the results are shown in (Fig. 2). In the FTIR spectrum of HA (Fig. 2A), broad peaks were observed at 3569.59 cm^{-1}, 3423.02 cm^{-1}, 2848.69 $cm^{-1,}$

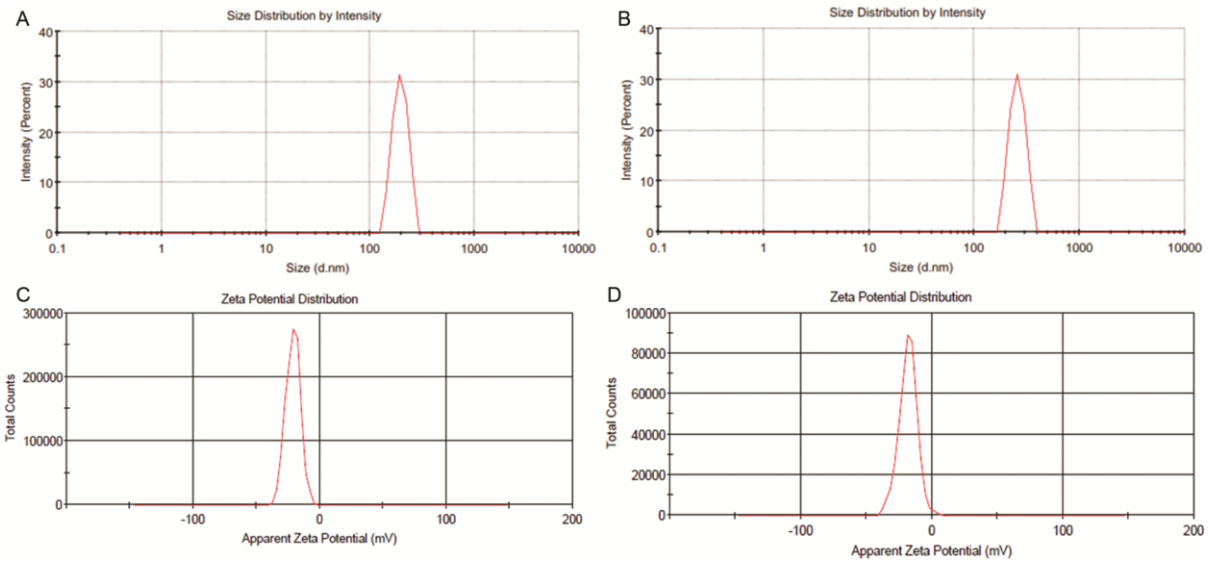

Fig. 1 — (A) DLS pattern of HA; (B) DLS pattern of HA-TP biocomposite; (C) Zeta potential of HA; and (D) Zeta potential of HA-TP biocomposite

and 2925.48 cm^{-1}, which corresponds to the characteristic stretching frequency of the O-H group and C-H stretching of the methyl esters. The peaks at 3569.59 and 3423.02 cm^{-1} are assigned to the absorbed moisture content on HA. The absorption band at 1648.83 cm^{-1} was attributed to the absorption of carboxylic groups and carboxylate. The peaks resulted from the slight bending mode of the P-O bond of PO_4^{3-} the group was found at 1085.72, 739.20, 603.2, 561.6, and 460.8 cm^{-1} (Fig. 2A). The intensities of these phosphate vibrations can be used as an indication of the crystallinity of the HA[29]. The observed results were compared and conformed to the previous reports of Varadarajan *et al*.[30] and Subramanian *et al*[31].

The FTIR spectrum of ethanolic TP extract was shown in (Fig. 2B). A broad and strong absorption band of the O-H group was found at 3399.88 cm^{-1}. The medium stretching mode of the C-H group of aldehyde was found at 2927.41 cm^{-1}. At 2138.66 cm^{-1}, the C=C alkyne group was identified. The active carboxylic group of compounds (C=O) was found at 1627.62 cm^{-1}. The band present in the 1405.85 cm^{-1} wavenumber shows the amide group compounds (N-H). The peaks at 1286.28 and 1068.37 cm^{-1} represent the C-N stretch of the amine group of plant chemical compounds. The spectral absorption peak at 624.82 cm^{-1} represents alkenes with C-H stretch. The functional groups C=C, C=O, and O-H are more prominent in the TP[32,33]. The FTIR result shows a variety of bands of varying intensities, indicating a high concentration of phytochemicals in the ethanolic TP leaves extract.

The FTIR spectrum of HA-TP biocomposite was shown in (Fig. 2C). The recorded spectrum of HA-TP biocomposite shows a similar structure as that of pure HA and TP with a slight change in the spectrum band wave numbers (495.61, 568.89, 611.32, 727.03, 1029.80, 1064.51, 1164.79, 1213.00, 1405.85, 1629.55, 2138.66, 2854.13, 2921.62, and 3397.95 cm^{-1}). Moreover, in the HA-TP biocomposite sharper peaks were observed with higher content of phosphate group of compounds, especially at 817.67, 941.09, and 977.77 cm^{-1}. Finally, the obtained FT-IR spectra have confirmed the formation of HA-TP biocomposite with no other impurities[34].

The XRD peaks pattern is notably sharper in HA and HA-TP biocomposite and found to be matched with standard JCPDS file number 09-432 (Fig. 3). The lattice plane number received for the 2θ value of HA and HA-TP biocomposite is (101, 200, 002, 102, 211, 202, 321, 004, 210, and 221). The plane (211) of HA and HA-TP composite was matched with regular HA to get the greatest intensity, which represents both materials completely free of impurities (chief inorganic phase). The crystal system has a high uniformity and is hexagonal in nature.

Further, the intensity of the HA-TP biocomposite peaks get decreases which indicates strongly the decrease in the crystallinity. The crystallinity of the synthesized HA nanoparticles is an important factor

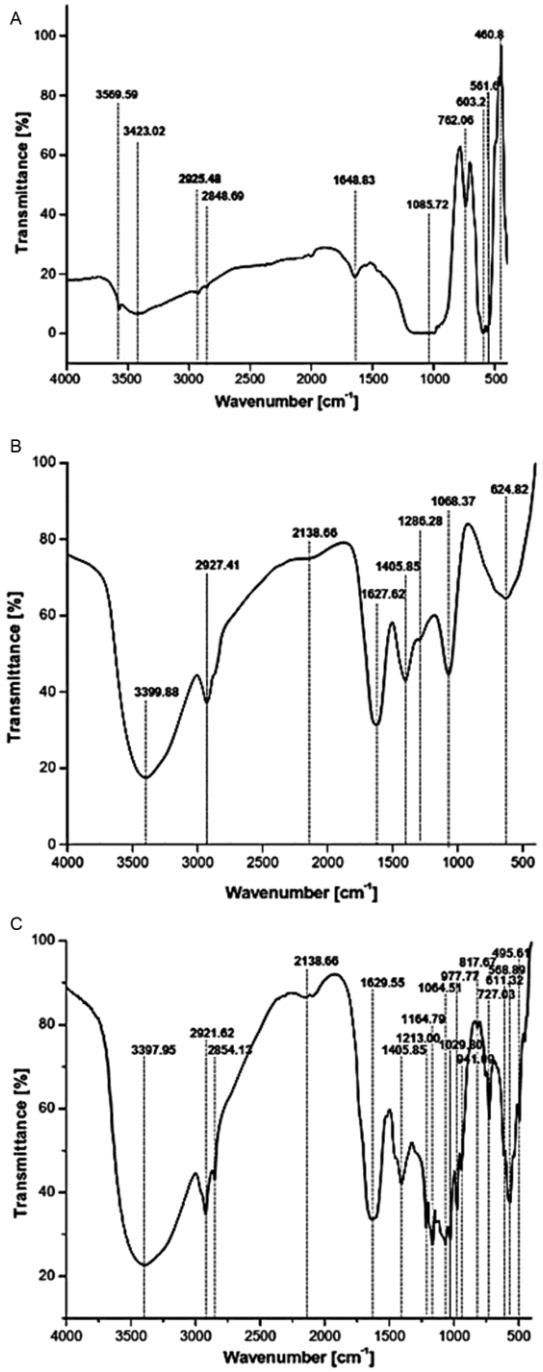

Fig. 2 — FTIR spectra of (A) HA; (B) TP; and (C) HA-TP biocomposite

for its biomedical uses. Generally, for biomedical purposes, the HA with low crystalline nature is needed due to its high *in vivo* resorbable property. Hence, the addition of TP has a significant effect on decreasing the crystalline nature of the as-synthesized HA-TP biocomposite. This observation is in accordance with previous reports where decreased

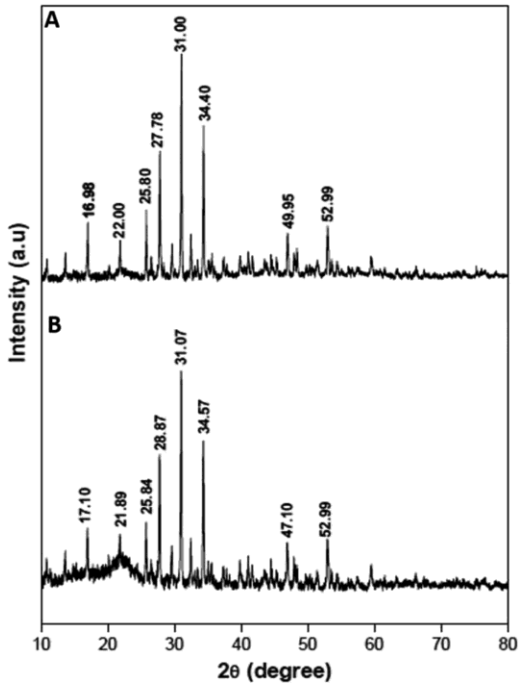

Fig. 3 — XRD pattern of (A) HA and (B) HA-TP biocomposite

crystallinity has been observed with other green-mediated hydroxyapatite composites[35,36].

The surface area and bioactivity of synthetic materials are largely influenced by their size and shape[37]. In SEM results, micrographs revealed the shape of HA and HA-TP biocomposite. It was found that the prepared HA and HA-TP biocomposite were spherical in shape and had a high-density crystalline structure, but that the HA-TP biocomposite had some aggregates (Fig. 4A & B). Ostwald ripening is an agglomeration process that occurs in solid solutions or liquid sols and explains the transformation of an inhomogeneous structure over time, in which small crystals or sol particles dissolve and redeposit onto larger crystals or sol particles[38]. The capping of the HA-TP biocomposite by the chemical ingredients contained in the extract of TP leaves could explain the slightly agglomerated form, which indicates the polydispersity in HA-TP biocomposite too[39].

HR-TEM analysis was also used to analyze the form and size distribution of the as-synthesized HA and HA-TP biocomposite (Fig. 4C & D). The HA and HA-TP biocomposite have an irregular form and a truncated distribution, according to these micrographs. The average diameter of the HA and HA-TP biocomposite is 16.57 – 64.22 nm and 51.71 – 138.68 nm, respectively. The capping of TP

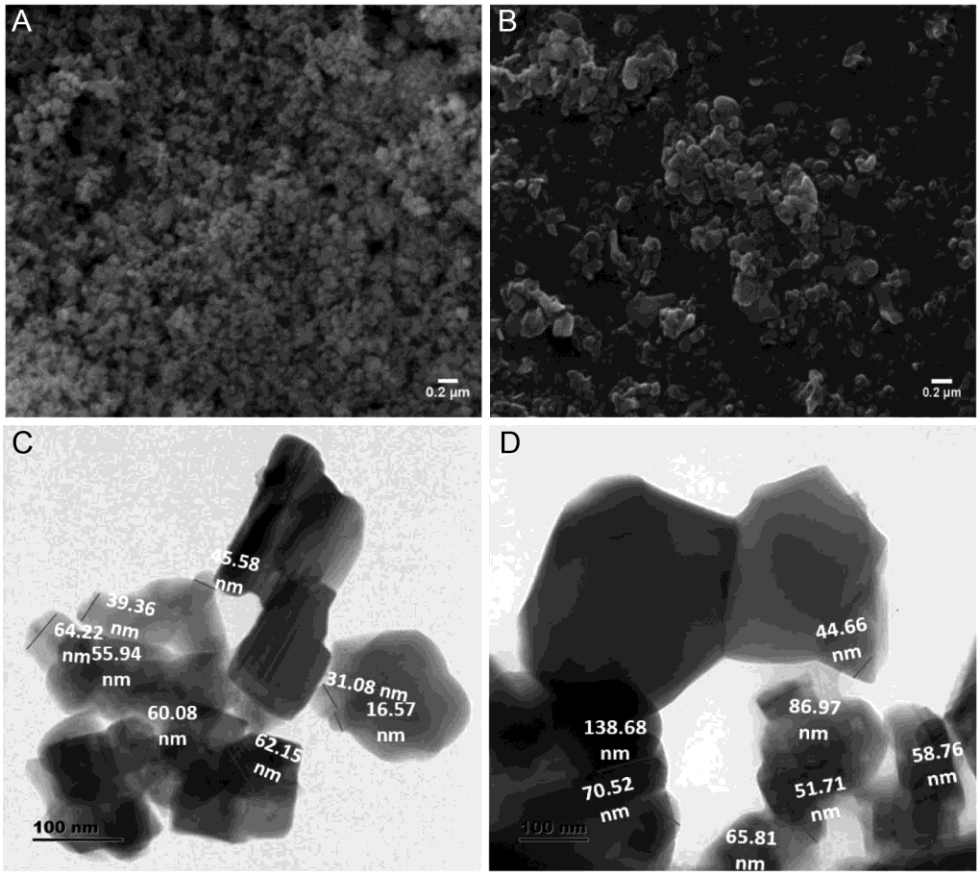

Fig. 4 — (A) SEM image of HA; (B) SEM image of HA-TP biocomposite; (C) HR-TEM image of HA; and (D) HR-TEM image of HA-TP biocomposite

phytomolecules into HA resulted in an increase in the size of the HA-TP biocomposite. The study found that a combination of HA and TP has resulted in an effective HA-TP biocomposite.

EDX analysis with elemental mapping was used to evaluate the elemental composition of HA, TP, and HA-TP biocomposite (Fig. 5A-C). The existence of oxygen, calcium, and phosphate atoms in pure HA was revealed, indicating the extreme purity of HA and the absence of any additional contaminants. In TP extract, carbon, oxygen, potassium, and chlorine were observed. In HA-TP biocomposite, oxygen, calcium, phosphate, carbon, potassium, and chlorine were noticed; at the same time, the calcium and phosphate ratio was gradually decreased by increasing plant extract concentration, which confirms that the biomolecules of plant extract were substituted in the host lattice of HA-TP biocomposite. Table 1 shows the different atomic proportions of as-synthesized HA, TP, and HA-TP biocomposite. This study too concluded that a combination of HA and TP resulted in an effective HA-TP biocomposite.

Table 1 — SEM-EDX chemical composition of HA, TP, and HA-TP biocomposite

Elements	HA	TP	HA-TP biocomposite
Ca (%)	29.02	—	16.20
P (%)	18.40	—	11.41
O (%)	42.83	24.61	45.13
C (%)	8.12	59.82	20.25
K (%)	—	9.95	4.01
Cl (%)	—	2.40	1.58
Al (%)	0.62	1.91	—
Total (%)	98.99	98.69	98.58

Antioxidant activity of HA-TP biocomposite

Recent research has highlighted the therapeutic potential of antioxidants present in natural products, demonstrating that they could be useful in managing the pathogenesis of chronic diseases. Specifically, anti-inflammatory and antioxidant substances have special benefits in reducing oxidative stress-induced damage, which is a hallmark of their pathophysiology. In the present study, the antioxidant potential of HA-TP biocomposite was unveiled by DPPH and ABTS

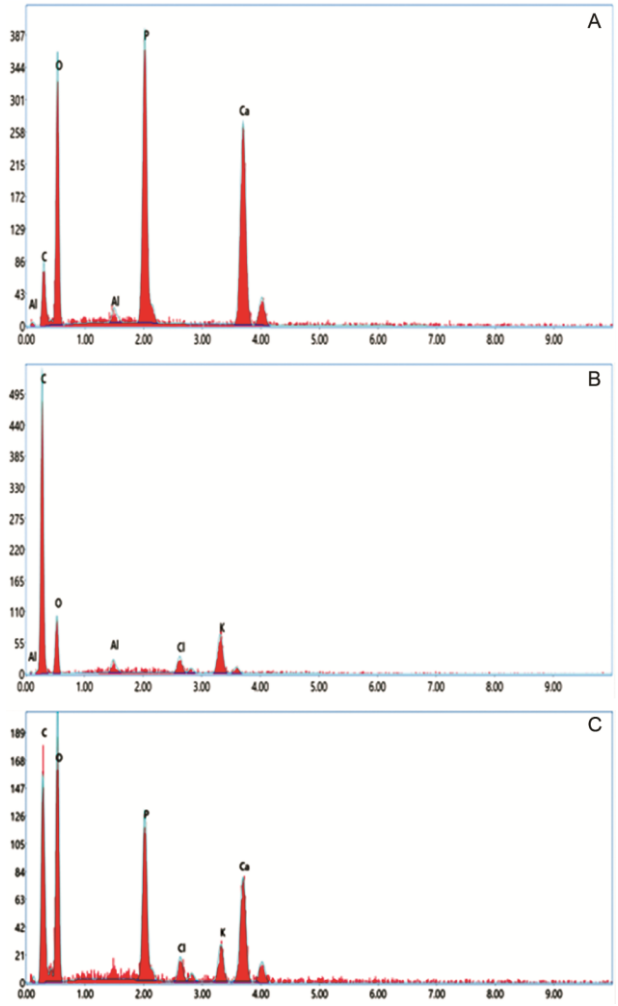

Fig. 5 — SEM-EDX pattern of (A) HA; (B) TP; and (C) HA-TP biocomposite

free radical scavenging assay. The antioxidant potential of HA-TP biocomposite was expressed as IC_{50} value, which means the amount of HA-TP biocomposite required to reduce the optical density of the DPPH and ABTS radical solution by 50%. In our study, HA-TP biocomposite has shown good antioxidant potential in DPPH and ABTS radical scavenging assays. The IC_{50} value of HA-TP biocomposite was determined as 156.69 ± 14.02 and 180.21 ± 12.84 µg/mL in DPPH and ABTS free radical scavenging assays, respectively. Sumathra *et al*. loaded plant component 6-gingerol into phosphorylated chitosan armed HA composite and observed DPPH radical scavenging activity up to 76.16%, which supports our findings[40]. According to the findings, as-synthesized HA-TP biocomposite could be extremely beneficial in the treatment of oxidative stress-related disorders.

Antimicrobial activity of HA-TP biocomposite

The most prevalent causes of the diseases include bacteria, viruses, protozoa, helminths, rickettsia, and fungus. With the introduction of β-lactam antibiotics, it was expected that infectious diseases, particularly bacterial illnesses, would no longer be a significant public health concern. However, with the rise of drug-resistant diseases, early optimism appears to have been misdirected. Scientists are working on a new class of antimicrobial agents that will target and eliminate drug-resistant infections[24]. Nanotechnology could be used to combat antimicrobial resistance, which could spur innovation and lead to the development of a new generation of antibiotic therapeutics for future medicines.

In the present study, a micro-well dilution technique was adopted to define the MIC and MBC of as-synthesized HA-TP biocomposite against pathogenic bacteria *S. aureus* – ATCC 13565 and *E. coli* – MTCC 41. The MIC and MBC of as-synthesized HA-TP biocomposite against *S. aureus* – ATCC 13565 were 181.09 ± 21.47 and 317.30 ± 41.03 µg/mL. Whereas, MIC and MBC of as-synthesized HA-TP biocomposite against *E. coli* – MTCC 41 were 157.59 ± 32.18 and 264.03 ± 21.58 µg/mL. The study concluded that as-synthesized HA-TP biocomposite demonstrated potent antimicrobial activity.

Crystal violet staining was used to demonstrate the antibiofilm ability of the as-prepared HA-TP biocomposite against pathogenic bacteria *S. aureus* ATCC 13565 and *E. coli* MTCC 41. The proportion of biofilm growth suppression by HA-TP biocomposite was calculated with respect to control (100%). The results demonstrated that the HA-TP biocomposite prevented biofilm development in the tested microbial pathogens in a dose-dependent manner. The MIC value of the HA-TP biocomposite showed superior inhibition of bacterial biofilm formation (Fig. 6A).

The images of antibiofilm activity of as-synthesized HA-TP biocomposite were shown in (Fig. 6B & C). The photos revealed that the bacterial biofilm was disturbed as the dose of HA-TP biocomposite was increased, and that this was dose-dependent. In support of our study, Jiang *et al*. loaded hydroxyapatite with β-tricalcium phosphate/calcium sulfate and successfully inhibited the biofilm formation in *P. aeruginosa* and *S. aureus*[41]. Similarly, Nica *et al*. doped hydroxyapatite coatings with samarium and demonstrated antibiofilm activity in an

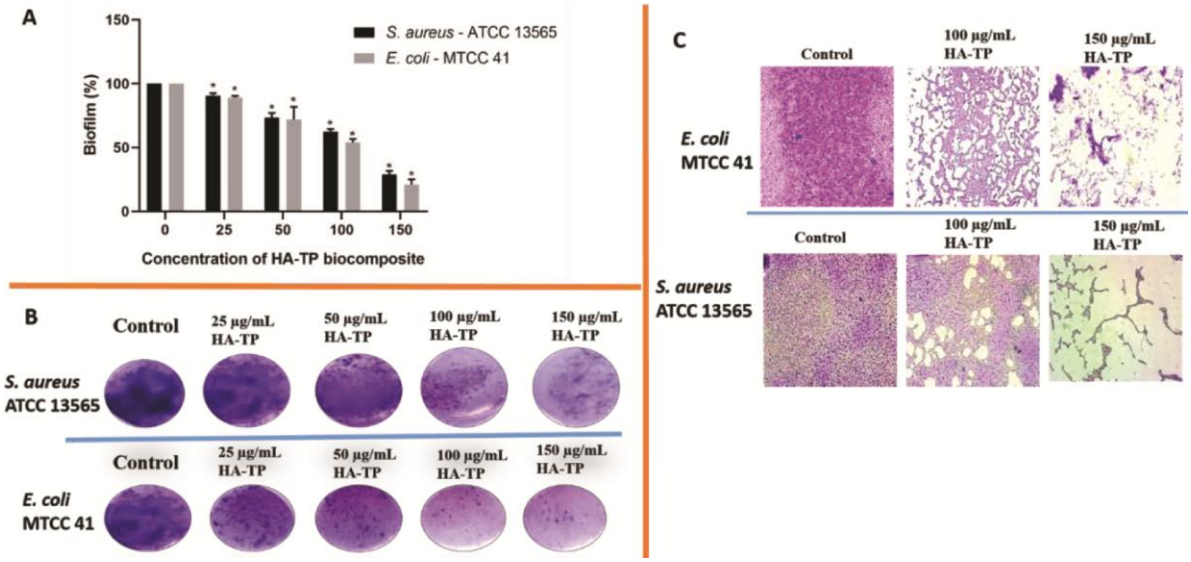

Fig. 6 — (A) Dose-dependent inhibitory effect of HA-TP biocomposite on biofilm formation. The statistical analysis between control and HA-TP biocomposite treated samples was assessed by Dunnett's test. The $P \leq 0.05$ was considered significant and denoted as '*'; (B) Crystal violet images of 24-well plates treated with different concentrations of HA-TP biocomposite against microbial pathogens; and (C) Microscopic images of microbial pathogens treated with different doses of HA-TP biocomposite. Images were captured at a magnification of 400X

in vitro study[42]. All of these discoveries, as well as the findings of this work, suggest that doped hydroxyapatite coatings could be excellent candidates for developing new antibacterial practices.

Conclusion

Ethanolic TP extract was found rich in phenolic, flavonoid, and tannin content and could be extremely beneficial in using the antioxidant potential for the treatment of oxidative stress illnesses. The as-prepared HA-TP biocomposite was successfully impregnated with TP extract and found to be stable, nanoscale, and crystalline. The HA-TP biocomposite showed antioxidant, and anti-biofilm properties. In the biomedical field, these features of the HA-TP biocomposite could be extremely beneficial in overcoming oxidative stress and microbial infections. Since the 1900s, the scientific community has been active in utilizing HA as a material for the development of bone and dental substitutes in orthopedic applications. In the last two to three decades, HA performance has much escalated by impregnating with metals and biomolecules. In recent times, HA has captivated the scientific community's interest, particularly in the optimization of three-dimensional, porous grafts, and bone-like scaffolds that mirror the trabecular architecture of human bone. Looking ahead, HA has raised expectations in orthopedic applications, which can be realized through sophisticated customized manufacturing methods, computer-aided design, physical simulation tools, *etc*.

Acknowledgement

Anusuya Nagaraj is thankful to DST-PURSE Phase-II, Bharathiar University, for providing fellowship and support. Naveen Kumar Kalagatur is thankful to SERB-DST, Government of India, for providing a national post-doctoral fellowship (NPDF).

Conflict of interest

All authors declare no conflict of interest.

References

1 Fiume E, Magnaterra G, Rahdar A, Verné E & Baino F, Hydroxyapatite for Biomedical Applications: A Short Overview. *Ceramics*, 4 (2021) 542.
2 Dubok VA, Bioceramics—yesterday, today, tomorrow. *Powder Metall Met Ceram*, 7 (2000) 381.
3 Mucalo M, *Hydroxyapatite (HAp) for biomedical applications*. (Elsevier) 2015.
4 Kattimani VS, Kondaka S & Lingamaneni KP, Hydroxyapatite–Past, present, and future in bone regeneration. *Bone Tissue Regen Insights*, 7 (2016) BTRI-S36138.
5 Zablotsky MH, Diedrich DL & Meffert RM, Detoxification of endotoxin-contaminated titanium and hydroxyapatite-coated surfaces utilizing various chemotherapeutic and mechanical modalities. *Implant Dent*, 1 (1992) 154.
6 Sundararaj N, Kalagatur NK, Mudili V, Krishna K & Antonysamy M, Isolation and identification of enterotoxigenic *Staphylococcus aureus* isolates from Indian

food samples: evaluation of in-house developed aptamer linked sandwich ELISA (ALISA) method. *J Food Sci Technol*, 56 (2019) 1016.

7 Li J, Xie S, Ahmed S, Wang F, Gu Y, Zhang C, Chai X, Wu Y, Cai J & Cheng G, Antimicrobial activity and resistance: influencing factors. *Front Pharmacol*, 8 (2017) 364.

8 Coelho CC, Araujo R, Quadros PA, Sousa SR & Monteiro FJ, Antibacterial bone substitute of hydroxyapatite and magnesium oxide to prevent dental and orthopaedic infections. *Mater Sci Eng C*, 97 (2019) 529.

9 Wang J, Wang L & Fan Y, Adverse biological effect of TiO_2 and hydroxyapatite nanoparticles used in bone repair and replacement. *Int J Mol Sci*, 17 (2016) 798.

10 Lakshmeesha TR, Kalagatur NK, Mudili V, Mohan CD, Rangappa S, Prasad BD, Ashwini BS, Hashem A, Alqarawi AA, Malik JA & Abd_Allah EF, Biofabrication of zinc oxide nanoparticles with *Syzygium aromaticum* flower buds extract and finding its novel application in controlling the growth and mycotoxins of *Fusarium graminearum*. *Front Microbiol*, (2019) 1244.

11 Lakshmeesha TR, Murali M, Ansari MA, Udayashankar AC, Alzohairy MA, Almatroudi A, Alomary MN, Asiri SM, Ashwini BS, Kalagatur NK & Nayak CS, Biofabrication of zinc oxide nanoparticles from *Melia azedarach* and its potential in controlling soybean seed-borne phytopathogenic fungi. *Saudi J Biol Sci*, 27 (2020) 1923-30.

12 Rajan M, Anthuvan AJ, Muniyandi K, Kalagatur NK, Shanmugam S, Sathyanarayanan S, Chinnuswamy V, Thangaraj P & Narain N, Comparative study of biological (*Phoenix loureiroi* fruit) and chemical synthesis of chitosan-encapsulated zinc oxide nanoparticles and their biological properties. *Arab J Sci Eng*, 45 (2020) 15.

13 Rao TCK, Rosaiah G, Mangamuri UK, Sikharam AS, Devaraj K, Kalagatur NK & Kadirvelu K, Biosynthesis of selenium nanoparticles from *Annona muricata* fruit aqueous extract and investigation of their antioxidant and antimicrobial potentials. *Curr Trends Biotechnol Pharm*, 16 (2022) 101.

14 Vundela SR, Kalagatur NK, Nagaraj A, Krishna K, Chandranayak S, Kondapalli K, Hashem A, Abd_Allah EF & Poda S, Multi-biofunctional properties of phytofabricated selenium nanoparticles from *Carica papaya* fruit extract: Antioxidant, antimicrobial, antimycotoxin, anticancer, and biocompatibility. *Front Microbiol*, 2 (2022) 4374.

15 Nagaraj A & Samiappan S, Presentation of antibacterial and therapeutic anti-inflammatory potentials to hydroxyapatite *via* biomimetic with *Azadirachta indica*: An *in vitro* anti-inflammatory assessment in contradiction of LPS-induced stress in RAW 264.7 cells. *Front Microbiol*, (2019) 1757.

16 Jachak SM, Gautam R, Selvam C, Madhan H, Srivastava A & Khan T, Anti-inflammatory, cyclooxygenase inhibitory and antioxidant activities of standardized extracts of *Tridax procumbens* L. *Fitoterapia*, 82 (2011) 173.

17 Salami SA, Salahdeen HM, Rahman OC, Murtala BA & Raji Y, Oral administration of *Tridax procumbens* aqueous leaf extract attenuates reproductive function impairments in L-NAME induced hypertensive male rats. *Middle East Fertil Soc J*, 22 (2017) 219.

18 Kalagatur NK, Kamasani JR & Mudili V, Assessment of detoxification efficacy of irradiation on zearalenone mycotoxin in various fruit juices by response surface methodology and elucidation of its *in vitro* toxicity. *Front Microbiol*, (2018) 2937.

19 Gunti L, Dass RS & Kalagatur NK, Phytofabrication of selenium nanoparticles from *Emblica officinalis* fruit extract and exploring its biopotential applications: antioxidant, antimicrobial, and biocompatibility. *Front Microbiol*, 10 (2019) 931.

20 Sanosh KP, Chu MC, Balakrishnan A, Kim TN & Cho SJ, Preparation and characterization of nano-hydroxyapatite powder using sol-gel technique. *Bull Mater Sci*, 32 (2009) 465.

21 Kumar KN, Venkataramana M, Allen JA, Chandranayaka S, Murali HS & Batra HV, Role of *Curcuma longa* L. essential oil in controlling the growth and zearalenone production of *Fusarium graminearum*. *LWT-Food Sci Technol*, 69 (2016) 522.

22 Kalagatur NK, Mudili V, Siddaiah C, Gupta VK, Natarajan G, Sreepathi MH, Vardhan BH & Putcha VL, Antagonistic activity of *Ocimum sanctum* L. essential oil on growth and zearalenone production by *Fusarium graminearum* in maize grains. *Front Microbiol*, 6 (2015) 892.

23 Kalagatur NK, Nirmal Ghosh OS, Sundararaj N & Mudili V, Antifungal activity of chitosan nanoparticles encapsulated with *Cymbopogon martinii* essential oil on plant pathogenic fungi *Fusarium graminearum. Front Pharmacol*, 9 (2018) 610.

24 Li J, Li S, Li H, Guo X, Guo D, Yang Y, Wang X, Zhang C, Shan Z, Xia X & Shi C, Antibiofilm activity of shikonin against *Listeria monocytogenes* and inhibition of key virulence factors. *Food Control*, 120 (2021) 107558.

25 Ghag SB & Ganapathi TR, Banana and plantains: improvement, nutrition, and health. In: *Bioactive molecules in food. Reference series in phytochemistry* (Ed. by JM Merillon, K Ramawat; Springer, Cham) 2018, 1.

26 George E, Kasipandi M, Venkataramana M, Kumar KN, Allen JA, Parimelazhagan T & Gopalan N, *In vitro* antioxidant and cytotoxic analysis of *Pogostemon mollis* Benth. *Bangladesh J Pharmacol*, 11 (2016) 148.

27 Kalagatur NK, Abd_Allah EF, Poda S, Kadirvelu K, Hashem A, Mudili V & Siddaiah C, Quercetin mitigates the deoxynivalenol mycotoxin induced apoptosis in SH-SY5Y cells by modulating the oxidative stress mediators. *Saudi J Biol Sci*, 28 (2021) 465.

28 Sharma K, Kumar V, Kaur J, Tanwar B, Goyal A, Sharma R, Gat Y & Kumar A, Health effects, sources, utilization and safety of tannins: A critical review. *Toxin Rev*, 40 (2021) 432.

29 Manatunga DC, de Silva RM, Nalin de Silva KM, de Silva N & Premalal EV, Metal and polymer-mediated synthesis of porous crystalline hydroxyapatite nanocomposites for environmental remediation. *R Soc Open Sci*, 5 (2018) 171557.

30 Varadarajan V, Varsha M, Vijayasekaran K & Shankar SV, Comparative studies of hydroxyapatite (HAp) nanoparticles synthesized by using different green templates. *AIP Conference Proceedings* (AIP Publishing LLC), 2020, 080002.

31 Subramanian R, Murugan P, Chinnadurai G, Ponmurugan K & Al-Dhabi NA, Experimental studies on caffeine mediated synthesis of hydroxyapatite nanorods and their characterization. *Mater Res Express*, 7 (2020) 015022.

32 Vijay R, Singaravelu DL, Vinod A, Sanjay MR, Siengchin S, Jawaid M, Khan A & Parameswaranpillai J, Characterization of raw and alkali treated new natural cellulosic fibers from *Tridax procumbens*. *Int J Biol Macromol*, 125 (2019) 99.

33 Rani R, Sharma D, Chaturvedi M & Yadav JP, Green synthesis of silver nanoparticles using Tridax procumbens: their characterization, antioxidant and antibacterial activity against MDR and reference bacterial strains. *Chem Pap*, 74 (2020) 1817.

34 Gayathri B, Muthukumarasamy N, Velauthapillai D & Santhosh SB, Magnesium incorporated hydroxyapatite nanoparticles: preparation, characterization, antibacterial and larvicidal activity. *Arab J Chem.*, 11 (2018) 645.

35 Gopi D, Kanimozhi K, Bhuvaneshwari N, Indira J & Kavitha L, Novel banana peel pectin mediated green route for the synthesis of hydroxyapatite nanoparticles and their spectral characterization. *Spectrochim Acta - A: Mol Biomol Spectrosc*, 118 (2014) 589.

36 Begum YA & Deka SC, Green synthesis of pectin mediated hydroxyapatite nanoparticles from culinary banana bract and its characterization. *Acta Aliment*, 46 (2017) 428.

37 Prabhu S & Poulose EK, Silver nanoparticles: mechanism of antimicrobial action, synthesis, medical applications, and toxicity effects. *Int Nano Lett*, 2 (2012) 1.

38 Thanh NT, Maclean N, Mahiddine S, Mechanisms of nucleation and growth of nanoparticles in solution. *Chem Rev*, 114 (2014) 7610.

39 Fatima F, Aldawsari MF, Ahmed MM, Anwer M, Naz M, Ansari MJ, Hamad AM, Zafar A & Jafar M, Green synthesized silver nanoparticles using *Tridax procumbens* for topical application: excision wound model and histopathological studies. *Pharmaceutics*, 13 (2021) 1754.

40 Sumathra M, Rajan M & Munusamy MA, A phosphorylated chitosan armed hydroxyapatite nanocomposite for advancing activity on osteoblast and osteosarcoma cells. *New J Chem*, 42 (2018) 12457.

41 Jiang N, Dusane DH, Brooks JR, Delury CP, Aiken SS, Laycock PA & Stoodley P, Antibiotic loaded β-tricalcium phosphate/calcium sulfate for antimicrobial potency, prevention and killing efficacy of *Pseudomonas aeruginosa* and *Staphylococcus aureus* biofilms. *Sci Rep*, 11 (2021) 1.

42 Nica IC, Popa M, Marutescu L, Dinischiotu A, Iconaru SL, Ciobanu SC & Predoi D, Biocompatibility and antibiofilm properties of samarium doped hydroxyapatite coatings: An *in vitro* study. *Coatings*, 11 (2021) 1185.